Large Reductions in Satellite-Derived and Modelled European Lower Tropospheric Ozone During and After the COVID-19 Pandemic (2020–2022)

Matilda. A. Pimlott[1], Richard. J. Pope[1,2], Brian. J. Kerridge[3,4], Richard. Siddans[3,4], Barry. G. Latter[3,4], Lucy. J. Ventress[3,4], Wuhu. Feng[1,5], Martyn. P. Chipperfield[1,2]

[1]School of Earth and Environment, University of Leeds, Leeds, LS2 9JT, UK

[2]National Centre for Earth Observation, University of Leeds, Leeds, LS2 9JT, UK

[3]Remote Sensing Group, STFC Rutherford Appleton Laboratory, Chilton, Oxfordshire, OX11 0QX, UK

[4]National Centre for Earth Observation, STFC Rutherford Appleton Laboratory, Chilton, Oxfordshire, OX11 0QX, UK

[5]National Centre for Atmospheric Science, University of Leeds, Leeds, LS2 9PH, UK

Key Points:

- The European satellite record shows large lower tropospheric spring-summer ozone reductions in 2020–2022 (8.4-14.6%).

- Scaling precursor emissions based on activity data yields large model ozone reductions in the spring-summer of 2020 and 2021.

- In 2020, meteorology contributed ~1/3 of the modelled reduction (low stratosphere-troposphere flux), with ~2/3 from emission reductions.

24 **Abstract**

25 Activity restrictions during the COVID-19 pandemic caused large-scale reductions in ozone (O_3) precursor

26 emissions, which in turn substantially reduced the abundance of tropospheric O_3 in the Northern Hemisphere.

27 Satellite records of lower tropospheric column O_3 (0 – 6 km) from the Rutherford Appleton Laboratory (RAL)

28 highlight these large reductions in O_3 during the COVID-19 period (2020), which persisted into 2021 and 2022. The

29 European domain average O_3 reduction ranged between 2.0 and 3.0 Dobson units (DU) (11.0-14.6%). These satellite

30 results were supported by the TOMCAT chemistry transport model (CTM) through several model sensitivity

31 experiments to account for changes in emissions and impact of the meteorological conditions in 2020. Here, the

32 business-as-usual (BAU) emissions were scaled by activity data (i.e. anonymised mobility data from big tech

33 companies) to account for the reduction in O_3 precursor emissions. The model simulated large O_3 reductions (2.0-3.0

34 DU), similar to the satellite records, where approximately 66% and 34% of the O_3 loss can be explained by

35 emissions changes and meteorological conditions, respectively. Our results also show that the reduced flux of

36 stratospheric O_3 into the troposphere accounted for a substantial component of the meteorological signal in the

37 overall lower tropospheric O_3 levels during the COVID-19 period.

38 **Plain Language Summary**

39 Lockdowns and other measures implemented to limit the spread of COVID-19 reduced human activity, leading to a

40 reduction in emissions from humans, including precursors for tropospheric ozone (O_3), a pollutant and greenhouse

41 gas. Studies have shown a reduction in tropospheric O_3 across the northern hemisphere in the spring-summer of

42 2020, which coincided with this emission reduction. We provide further evidence of the tropospheric O_3 reduction in

43 2020, specifically for Europe, using two records derived from satellite instruments. The two records show large

44 reductions in European tropospheric O_3 in the spring-summer of 2020, peaking at ~ 10 – 20 % in May. We use a

45 chemical transport model to distinguish between the impacts of emissions and meteorology in 2020–2021. In both

46 years, emission reductions had greater influence on the O_3 reduction (~2/3), highlighting the importance of

47 emissions in decreasing O_3. However, emissions reductions alone were not responsible for the large O_3 reduction, as

48 there was considerable influence from meteorology (~1/3), mostly from variation in the flux of O_3 from the

49 stratosphere.

50 **1 Introduction**

51 Tropospheric O_3 is an important secondary atmospheric pollutant and short-lived climate forcer, formed in the

52 presence of the precursor gases, nitrogen oxides (NO_x, referring to nitrogen dioxide (NO_2) and nitric oxide (NO))

53 and volatile organic compounds (VOCs), and sunlight (P. S. Monks et al., 2015). Tropospheric O_3 is a persistent

54 health problem in Europe, with 24,000 premature deaths attributed to acute O_3 exposure in 2020 (European

55 Environment Agency, 2022). O_3 is also the 3rd most important greenhouse gas, with an estimated effective radiative

56 forcing of 0.47 W m^{-2} (0.24–0.71 W m^{-2}) between 1750–2019, dominated by changes in tropospheric O_3 (IPCC,

57 2021; Skeie et al., 2020).

58

59   Due to a global pandemic caused by COVID-19 (disease from SARS-CoV-2, severe acute respiratory syndrome

60   coronavirus-2), many countries worldwide implemented a 'lockdown' of daily life activities to prevent the spread of

61   the disease (Forster et al., 2020; WHO, 2020; Zhou et al., 2020). This resulted in a widespread reduction in

62   anthropogenic surface emissions, including O_3 precursor gases. Based on activity data, Forster et al. (2020)

63   estimated a global reduction of ~ 30% for NO_x, 25% for carbon monoxide (CO) and 20% for VOCs in April 2020

64   and Guevara et al. (2021) estimated reductions of ~ 33% for NO_x and 8% for VOCs in March/April 2020. Here, the

65   changes in activity data reported by Forster et al., (2020) are based on changes in anonymised mobility data (e.g.

66   from phone GPS information) provided by Apple and Google (see Forster et al., (2020) and references within).

67   Typically, they found these mobility datasets used in their study to be within 20% of each other and had a

68   correlation of 0.8 or higher. Furthermore, Guevara et al. (2021) found that countries with the severest lockdowns had

69   even higher average reductions (~ 50% for NO_x, 14% for VOCs).

70

71   Reductions in tropospheric O_3 in the spring-summer across the northern hemisphere (NH) free troposphere (FT) was

72   initially described by Steinbrecht et al. (2021). The timing of this reduction coincides with the introduction of

73   lockdowns across Europe, beginning in the spring-summer of 2020 and continuing into 2021. Steinbrecht et al.

74   (2021) found that in 2020, measurements of the NH FT (mostly from ozonesondes) from April–August showed ~7%

75   lower O_3 values, compared to its climatology of 2000–2020. Such a widespread reduction occurring at so many

76   stations had not occurred previously in this time period. Another notable event during winter-spring of 2019/2020

77   was the very large stratospheric Arctic O_3 depletion caused by a very cold, strong and long-lasting polar vortex (W.

78   Feng et al., 2021; Weber et al., 2021; Wohltmann et al., 2020). Steinbrecht et al. (2021) suggested that this low

79   stratospheric O_3 event contributed to less than 25% of this O_3 negative anomaly, attributing most of the O_3 reduction

80   to emission reductions. Further studies have confirmed low FT O_3 across Europe and the NH using aircraft and

81   ozonesonde measurements (e.g. Chang et al. (2022); Clark et al. (2021); Putero et al. (2023). In contrast, Parrish et

82   al. (2022) suggested that low 2020 tropospheric O_3 could be largely due to a negative trend in baseline tropospheric

83   O_3 since around the mid-2010s, based on Western European surface sites.

84

85   From a satellite perspective, Ziemke et al. (2022) found low NH spring-summer FT O_3 from instruments aboard

86   NASA satellites, using a merged instrument record. The tropospheric column O_3 reduction of ~ 7–8% (3 DU)

87   (compared to 2016–2019), was comparatively uniform between 20°N - 60°N and repeated in the next year, 2021.

88   They found a reduction of NH satellite-derived NO_2 (~ 10–20%) in the spring-summer of 2020 and 2021, attributing

89   this as the likely cause of the O_3 reduction. Cuesta et al. (2022) found that satellite-derived lowermost tropospheric

90   O_3 (< 3 km altitude) in the spring (1st–15th April) of 2020 was enhanced across central Europe and northern Italy

91   (typically VOC-limited regions) compared to the previous year (2019) and reduced elsewhere in Europe (typically

92   NO_x-limited regions). An enhancement of O_3 across central Europe in the spring-summer of 2020 was also found at

93   surface monitoring sites (e.g. Ordóñez et al. (2020); Grange et al. (2021)). Apart from Ziemke et al. (2022), there are

94   few studies of 2021 and onwards. One example is from Pey & Cerro (2022), finding reduced background O_3 values

95   over SW Europe (~15% at most sites) in March-April 2020, which was also seen in 2021 but to a lesser extent.

96   Similar results were found in the study by Dunn et al., (2024).

97

98   Modelling studies have investigated the impact of emission reduction on FT O_3, using different methods to estimate

99   the size of these emission reductions, which are still uncertain. Bouarar et al. (2021) modelled primary pollutant

100   emission reductions, based on emission reductions from activity data by Doumbia et al. (2021), finding zonally

101   averaged NH FT O_3 to be reduced by 5–15% (2001–2019 baseline). One third of this reduction is attributed to

102   reductions in air traffic, one third is attributed to a reduction in surface emissions and the final third is attributed to

103   meteorology, including the low 2020 springtime Arctic stratospheric O_3. Miyazaki et al. (2021) used data

104   assimilation, finding a reduction in the global tropospheric O_3 burden of ~ 2% in May and June 2020.

105

106   Here, we present an update to the European tropospheric O_3 record using two satellite products, extending the record

107   to mid-2023, and present the reductions in the lower FT compared to previous years. Using a 3-D chemical transport

108   model, TOMCAT (Monks et al., 2017), we explore the impact of scaling the anthropogenic surface emissions (from

109   activity data changes) on European tropospheric O_3 in 2020 and 2021. Lastly, we quantify the relative contribution

110   of emissions and meteorology to the modelled reduction in tropospheric O_3.

111   **2 Data and Methods**

112   2.1 Tropospheric Ozone Satellite Datasets

113   We present satellite-derived O_3 from two satellite instruments, the Infrared Atmospheric Sounding Interferometer

114   (IASI) and the Global Ozone Monitoring Experiment-2 (GOME-2), both aboard EUMETSAT's satellite MetOp-B

115   (Clerbaux et al., 2009; Munro et al., 2016). The MetOp series of satellites have a sun-synchronous, near polar orbit

116   with an equator crossing time of 9:30 local solar time (LST). IASI has a swath width of 2200 km, and in the nadir

117   viewing mode, there are four circular fields of view across-track with a diameter of 12 km, covering a square $50 \times$

118   $50 \ km^2$ which is scanned across the swath. IASI measures in the infrared (IR) wavelengths (645–2760 cm^{-1}) with a

119   spectral resolution of 0.3 - 0.5 cm^{-1} (Clerbaux et al., 2009). GOME-2 measures in the ultraviolet-visible (UV-Vis)

120   wavelengths (240–790 nm) with a spectral resolution of 0.26 - 0.51 nm, and has a swath width of 1920 km. The field

121   of view is scanned across-track yielding 24 ground-pixels of dimension 80 km (across-track) $\times$ 40 km (along-track)

122   (Callies et al., 2000; Munro et al., 2016). For quality assurance, the GOME-2B record was filtered for a geometric

123   cloud fraction of <0.2 (e.g. Miles et al. (2015)) and the IASI-IMS-extended record was filtered for an effective cloud

124   fraction of <0.5 (as in Pope et al. (2021)). Here, the RAL Space GOME-2 and IASI Infrared and Microwave

125   Sounding (IMS) retrieval schemes for lower tropospheric ozone have been independently evaluated against

126   ozonesonde data in Miles et al., (2015) and Pimlott et al., (2022).

127

128   Height-resolved O_3 distributions are retrieved by the Rutherford Appleton Laboratory (RAL) using the IMS-

129   Extended scheme for IASI (detailed in Pope et al. (2021)) and UV-Vis scheme for GOME-2 (detailed in Miles et al.

130   (2015)). Due to an underlying negative tendency in the GOME-2 record, likely from UV degradation of the

instrument, we have detrended that record, as shown in **Supplement Text S1** and **Figure S1**. To compare the IASI-IMS-Extended data from MetOp-B (2018–2023) to a longer time-period, we combine the record with IASI-IMS-Extended data from MetOp-A (2008–2017). The MetOp-B record was adjusted according to monthly differences with the MetOp-A record in the overlap year of 2018, as described in **Supplement Text S2** and **Figures S2 and S3**. Here we use lower tropospheric sub-columns of the surface–450 hPa (~6 km altitude) derived from the retrieved profiles, with a focus on Europe. As such, we use a land mask to extract a terrestrial European signal given the direct link between surface O_3, precursors gases and air pollution exposure (see **Supplement Figure S4**).

2.2 Model Simulations

We use the TOMCAT 3-D chemical transport model to simulate tropospheric O_3 between 2017 and 2021. The model control simulation is for 2017, 2018 and 2019. However, in 2020, the control simulation splits into two scenarios: 1) business-as-usual scenario (BAU) and 2) scaled emission scenario (COVID). For the BAU scenario, the control modelled emissions inventory is used but for the COVID scenario, we apply emission reduction factors (Forster et al., 2020) to model surface and aircraft emissions to account for changes in activity due to the pandemic in 2020 and 2021. However, COVID scaling for emissions are not available beyond 2021, so the model simulations are restricted to 2017-2021. TOMCAT is an off-line model driven by 6-hourly ERA-5 meteorological reanalyses (e.g. temperature, relative humidity, winds; Hersbach et al., 2020), which are provided by the European Centre for Mid-Range Weather Forecasting (ECMWF). The ERA-5 meteorological reanalyses are provided on 137 vertical levels (surface to 1 hPa), which are interpolated onto the TOMCAT vertical grid (31 levels -see Monks et al., (2017) Figure 1). It has a horizontal a resolution of $2.8° \times 2.8°$ and 31 vertical levels between the surface and 10 hPa, coupled with the Global Model of Aerosol Processes (GLOMAP) (Chipperfield, 2006; Mann et al., 2010; Spracklen et al., 2005). The chemistry scheme includes approximately 80 advected tracers and over 200 chemical reactions (S. A. Monks et al., 2017).

Surface emission fields are described in detail in **Supplement Text S4** and **Table S1**. The anthropogenic emissions are from the Coupled Model Intercomparison Project Phase 6 (CMIP6) (L. Feng et al., 2020), whereby after 2014 emissions are based on Shared Socioeconomic Pathways (SSPs) (Gidden et al., 2019; Riahi et al., 2017). In this study, we have used the middle-of-the-road scenario, SSP2-4.5, for the TOMCAT control run between 2017 and 2019, before diverging into the BAU and COVID simulations. For the BAU simulation, the CMIP6 SSP2-4.5 emissions are used but for the COVID simulation, scaling factors for emission reductions from national lockdowns come from Forster et al. (2020) and were applied to the BAU emissions. Forster et al. (2020) used national mobility/activity data to estimate reductions in air pollutant emissions (i.e. NO_x, CO, VOCs, black carbon (BC) and organic carbon (OC)). **Figure 1(a)** highlights the impacts of the scale factors, with substantial decreases evident in European emissions for NO_x, CO and VOCs. **Figure 1(b)** shows that the peak reductions were in April 2020, once most European lockdowns were in effect, with monthly reductions of 0.44 Tg (33%), 0.75 Tg (34%) and 0.06 Tg (29%) of NO_x (as NO_2), CO and NMVOCs (as carbon (C)), respectively. For 2020, a secondary winter emissions reduction occurs at ~ 15–20% as further European lockdowns were imposed to reduce the spread of COVID-19. For

167   2021, the scaling factors from Forster et al. (2020) suggest that emissions were approximately 10–13% lower than

168   expected but remained consistent throughout the year, suggesting a potential 'new normal' of lower precursor

169   emissions. A tracer for stratosphere-troposphere exchange (STE) in the model (O_{3S}) is used to understand the impact

170   of O_3 transport from the stratosphere. In the stratosphere, it is set equal to the model-calculated O_3. The only

171   tropospheric source of the tracer is transport from the stratosphere while its sinks are via photolysis, surface

172   deposition and reactions with HO_2, OH and H_2O through $O(^1D)$ produced from O_{3S} (S. A. Monks et al., 2017).

173

174   Overall, TOMCAT is a robust and well evaluated CTM having been used in multiple studies of tropospheric O_3 and

175   compared with many types of observation (e.g. Richards et al., (2013), Pope et al., (2020) and Pope et al., (2023,

176   2024). The simulated tropospheric ozone burden is a common metric to assess the skill of a model to simulate

177   tropospheric ozone. Here, we derive a tropospheric O_3 burden of 322 Tg (BAU 2020 simulation), which is

178   consistent with that of Monks et al., (2017) who reported an equivalent of 331 Tg. Both estimates sit within the

179   reported range of 337±23 Tg from the Atmospheric Chemistry and Climate Model Intercomparison Project

180   (ACCMIP, Young et al., 2013) further demonstrating TOMCAT to be a suitable modelling framework. Highly

181   relevant for this work, Pope et al., (2023) included a detailed comparison of lower tropospheric ozone between

182   TOMCAT and GOME-2/IASI, where thorough consideration of the satellite averaging kernels (i.e. function of

183   satellite vertical sensitivity when retrieving sub-column profiles of O_3) was taken in conjunction with the model,

184   generally displaying good agreement with the between them. Therefore, we are confident in using TOMCAT to

185   directly investigate the impact of COVID-19 on lower tropospheric ozone over Europe.

186
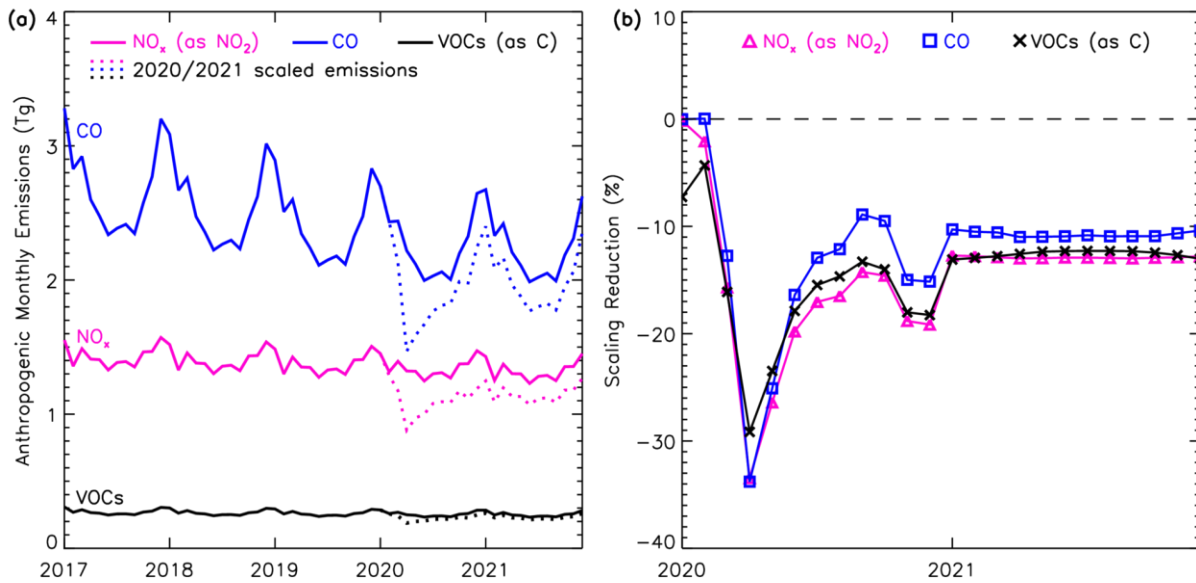
187   **Figure 1.** European aggregated anthropogenic monthly emissions of NO_x (as NO_2), CO and NMVOCs (as C) used
188   in the TOMCAT simulations between 2017 and 2021. (a) BAU emissions (solid) and COVID emissions in 2020 and
189   2021 (dotted) (Tg). (b) Percentage reduction in 2020 and 2021 for NO_x, CO and VOCs in the COVID emissions,
190   relative to the BAU emissions.

3 Results and Discussion

3.1 European Tropospheric Ozone Satellite Record (2008–2023)

We present two satellite-derived lower tropospheric sub-column O_3 records for continental Europe from 2008–2023 (**Figure 2**). During the overlapping years of 2015–2019, the records show an average difference of 2.5 DU, but the variability is well correlated (Pearson's correlation coefficient ~ 0.80). Satellite record inconsistencies are likely due to differences between IR and UV-Vis instruments, the related retrieval schemes and their vertical sensitivities, despite the instruments being aboard the same platform and having the same overpass time. Compared to a monthly baseline of 2015–2019 for GOME-2B and 2008–2019 for IASI-IMS-Extended, the monthly anomalies (**Figure 2(b)**) show good agreement through this overlap period, with the most notable disagreements in winter/spring of 2015 and spring-summer 2016. Both records show large negative anomalies in spring-summer 2020. GOME-2B shows peak negative anomalies of 2.4 DU (18.3%) and 3.0 DU (21.4%) in April and May 2020, respectively, and IASI-IMS-Extended shows slightly smaller negative anomalies of 1.7 DU (9.4%) and 2.2 DU (11.0%) in April and May, respectively. For the records shown in **Figure 2(b)**, two standard deviations (2σ) across the entire monthly record is 2.1 DU for GOME-2B and 1.8 DU for IASI-IMS-Extended. Thus, ~ 95% of the data ranges between the average $\pm 2\sigma$ for the respective records. In both cases, April and May 2020 negative anomalies either match or surpass this range signifying relatively substantial anomalies for these months, highlighting their unusual nature. The reductions continue into the summer of 2020, with both records showing large negative anomalies in July and August: 1.7 DU (9.2%) and 1.4 DU (7.2%) for GOME-2B; 1.8 DU (8.3%) and 1.3 DU (6.3%) for IASI-IMS-Extended.

Tropospheric O_3 reductions continue into the spring and summer period of 2021, with the IASI-IMS-Extended record showing negative anomalies in most months of 2021, however, these anomalies are slightly smaller than in 2020. The largest negative anomalies are in April, May and June, at 1.0 DU (5.3%), 1.7 DU (8.4%) and 1.1 DU (5.2%), respectively, with only the reduction in May being close to the average $\pm 2\sigma$ threshold. This recurrence in 2021 of a tropospheric O_3 reduction of similar magnitude to 2020 is consistent with the combined NASA satellite product tropospheric column O_3 record for the 20-60N latitude band reported by Ziemke et al. (2022), which is presented from January–August.

It is worth noting that there is approximately a 1-month lag between the IASI and GOME-2 time-series in Figure 2 which is likely due to the European domain (see Figure S4 of the Supplement) extending to high northern latitudes (approximately 70°N) where sampling of the GOME-2 UV sounder, but not IASI, is restricted in winter months by absence of sunlight. While this could slightly influence the domain average annual cycle comparison it does not affect the interannual variability subject of this study.

In 2022, the IASI-IMS-Extended record shows even larger negative anomalies in April and May than 2020/2021, of 2.6 DU (15.0%) and 2.8 DU (14.6%), respectively, which are well beyond the average $\pm 2\sigma$ threshold. The negative

227   anomalies continue in June and July, with 1.3 DU (6.5%) and 1.3 DU (6.1%). In 2023, the negative
228   spring-summer are smaller compared to 2020–2022, apart from in May, where the negative anomaly is 1.3 DU
229   (6.1%). Broadly, the years of 2020–2023 all show monthly anomalies which are more consistently negative than the
230   previous 12 years. The question of the persistence of low European O_3 values will become evident in future years
231   through extension of these MetOp records.
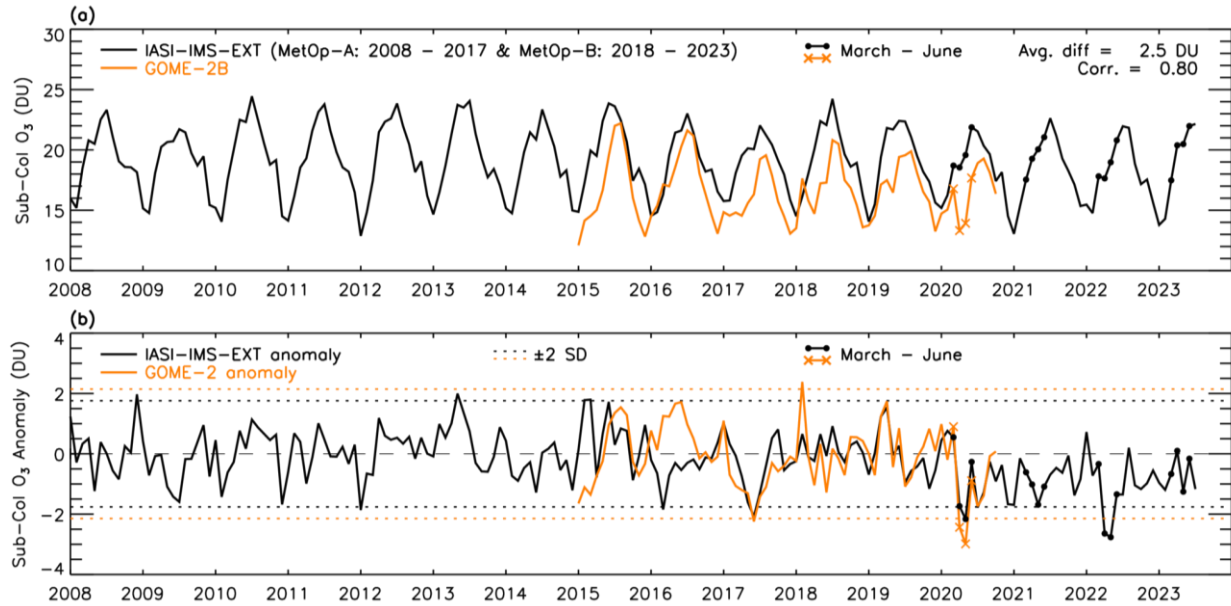
233   **Figure 2.** European satellite-derived O_3 from January 2008–July 2023. (a) Monthly average sub-column (surface–
234   450 hPa) O_3 record (DU) from IASI (IASI-IMS-extended, January 2008–July 2023) and GOME-2B (January 2015–
235   October 2020). (b) Monthly mean anomalies for the two records (2015–2019 baseline for GOME-2B, 2008–2019
236   for IASI-IMS-Extended) (DU). Dotted lines indicate ± 2σ from the average of the record. Filled circles (IASI-IMS-
237   Extended) and crosses (GOME-2B) are shown for the months of March–June in 2020–2023, to highlight the
238   relevant spring/summer periods. Average difference and correlation are based on January 2015–December 2019.

239   3.2 TOMCAT Model Experiments (2017–2021)

240   In 2020, scaling the emissions according to the mobility data estimates in Forster et al. (2020) (TOMCAT COVID
241   scenario) caused a monthly reduction in tropospheric O_3 from March to December (**Figure 3(a)**). During January
242   and February, the COVID and BAU scenarios are very similar, however, from March onwards the COVID scenario
243   shows a negative difference compared to the BAU scenario, which peaks at 2.0 DU (8.3%) lower in May. This
244   negative difference then reduces through the year to December (0.7 DU, 4.1%). **Figure 4a** shows the spatial impact
245   of COVID-19 on lower troposphere ozone simulated by TOMCAT. The March-May 2020 average is typically 1.0-
246   2.0 DU lower across the whole European domain. In 2021, the COVID scenario in Figure 3(a) shows consistent
247   reductions in all months of the year, starting at 0.6 DU (3.4%) in January, peaking at 1.0 DU (4.3%) in May, and
248   reducing towards the end of the year, ending with 0.6 DU (3.2%) in December. The temporal pattern of the
249   reduction is similar to that in surface emissions (**Figure 1**), although with considerably smaller percentage decreases
250   (peak of ~30% for surface emissions and ~8% for the resulting O_3 sub-column). This highlights the large emission
251   reductions required for a sizeable reduction in European lower tropospheric O_3. To identify the impact of

8

252 meteorology in 2020, the scaled emissions in 2020 were used in three separate simulations with the meteorology of
253 2017, 2018 and 2019, with an average of these three scaled emission simulations shown in **Figure 3(b)**. The 2020
254 COVID scenario record is broadly lower than the 2017/2018/2019 averaged scaled emission scenario, despite using
255 the same surface emissions, which indicates that the meteorology of 2020 had a large impact on the tropospheric O_3
256 reduction. Here, we use the term "meteorology" to represent meteorological variables such as temperature, pressure
257 and humidity, but also the long-range transport (i.e. advection/convection) of air masses, which influence
258 tropospheric chemistry. This is supported by **Figure 4b** which shows that across most of Europe, 2020
259 meteorological conditions where more conducive to lower tropospheric ozone loss (i.e. differences of -3.0 and -1.0
260 DU) than previous years. However, the domain average shown for March-May 2020 in **Figure 3b** is buffered by the
261 positive differences (up to 1.0-1.5 DU) above $60^\bullet N$. The impact of meteorology in 2020 is greatest in the spring-
262 summer (**Figure 3b**), as the differences between these two timeseries is largest from February–July, peaking at a 1.1
263 DU difference in May. This demonstrates the importance of meteorology to the resulting O_3 in the spring-summer of
264 2020. The records are much more consistent from August to the end of the year, with absolute differences below 0.6
265 DU, indicating a reduced impact from meteorology in the second half of the year.
266
267 In comparison with the previous 3 years (2017–2019), the BAU scenario in 2020 and 2021 has lower peak spring-
268 summer values of O_3, especially compared to the high O_3 values in 2019 (**Figure 3(a)**). The spring-summer of 2020
269 shows negative anomalies in the BAU scenario of up to 1.4 DU (-5.8%) (**Figure 3(c)**). April, May and July show the
270 largest reductions, which are around the value of the average $\pm 2\sigma$ threshold (± 1.3 DU, 6.2%). The spring-summer
271 BAU scenario reductions are repeated in 2021 from January–June, peaking at 1.2 DU (4.9%) in May. Any variation
272 in the BAU scenario is due to meteorology and also variation in the BAU surface emissions used. As shown in
273 **Figure 1**, the BAU emissions only vary by a small amount from year to year, e.g. the average total annual
274 anthropogenic emission difference between consecutive years across the simulation time period is 0.33 Tg (2.0%)
275 for NO_x, 1.3 Tg (4.4%) for CO and 0.06 Tg (1.8%) for VOCs. With consistent BAU emissions, meteorology is the
276 dominant control in the BAU scenario and had a large impact on the simulated tropospheric O_3 in the spring and
277 summer of 2020.
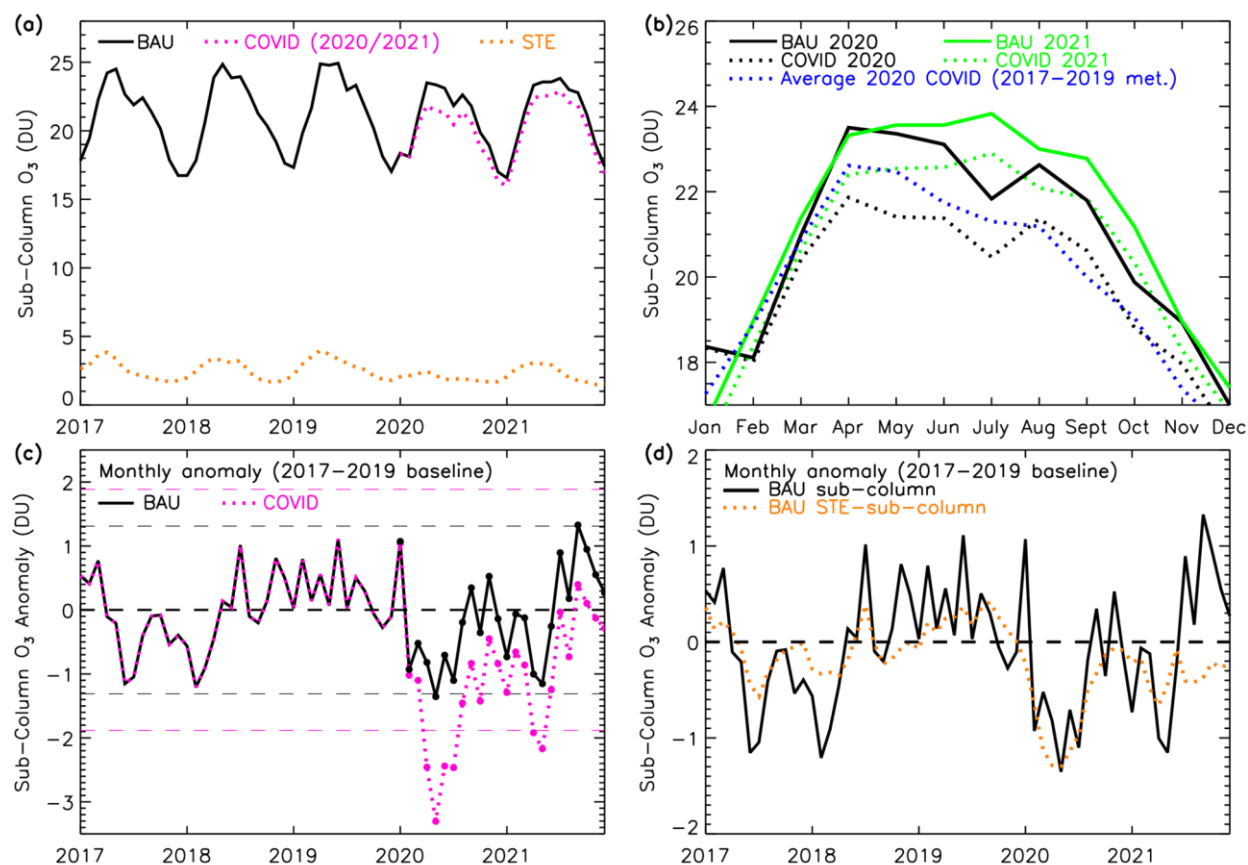
Figure 3. TOMCAT European lower tropospheric sub-column O_3 (surface–450 hPa) between 2017 and 2021 (DU). (a) Monthly sub-column O_3 averages for the BAU sub-column (solid, black) and STE-contribution sub-column (dotted, orange). The COVID scenario is shown in 2020 and 2021 (pink dotted). (b) BAU (solid, black) and COVID scenario (dotted) records for 2020 (black), 2021 (green), with the 2017/2018/2019 averaged COVID scenario (2020 scaled emissions, dark blue, dotted). (c) BAU (solid, black) and COVID (pink, dotted) O_3 anomalies (baseline of 2017–2019). Horizonal dashed lines indicate $\pm 2\sigma$ from the average of the record. (d) As panel (c) with the inclusion of monthly O_3 anomalies of the stratosphere-troposphere exchange (STE)-contribution sub-column (orange, dotted).
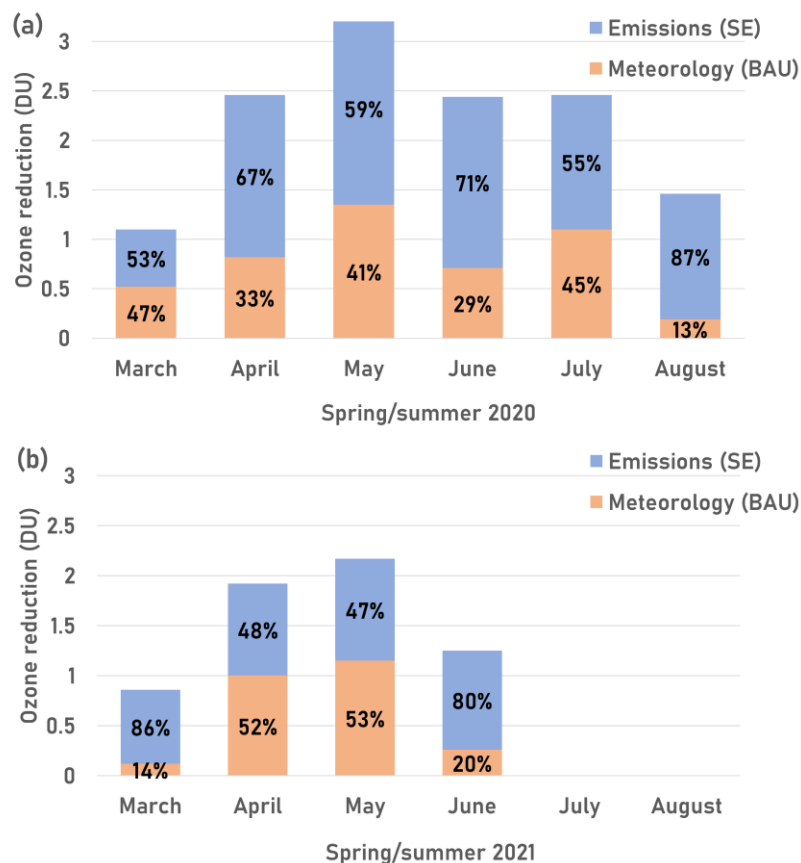
The COVID scenario shows large negative anomalies in 2020, peaking at 3.3 DU (15.4%) in May 2020 (**Figure 3c**), which is much more than the average $\pm 2\sigma$ threshold (± 1.9 DU, 9.0%). Comparing the BAU and COVID scenarios suggests that ~1 DU of the negative anomaly is due to meteorology (and small variations in BAU emissions) and the remaining contribution (~ 1–2 DU in spring-summer) of the negative anomaly is due to the scaled emissions for 2020. The contribution of O_3 from STE to the troposphere in the model sub-column is calculated by TOMCAT as a tracer which represents stratospheric O_3 that has entered the troposphere and is controlled by tropospheric sink processes. We calculate a sub-column based on this contribution (STE-sub-column), shown in **Figure 3(a)**, varying between 1.5–4.0 DU from 2017–2021. We find a large negative anomaly in model stratosphere-troposphere O_3 exchange (STE) in the spring-summer of 2020 (**Figure 3(d)**), of 1.3 DU in both April and May (52.5% and 60.5%, respectively). The STE-sub-column absolute negative anomaly is a similar value or larger than the lower tropospheric sub-column anomaly from March - August in 2020, suggesting that during this period, low STE

298   contribution was a substantial factor in the BAU scenario lower tropospheric sub-column O_3 reduction. In the

299   months where the STE-sub-column absolute anomaly is larger than the BAU anomaly, the other controlling factors

300   in the BAU simulation O_3 are likely around neutral or even slightly positive. The stratospheric O_3 used in the model

301   simulation is a climatology, therefore, any variation on the STE contribution is from variation in the STE flux. In

302   2021, the negative anomaly in STE-sub-column is smaller than for 2020, reaching a peak value of 0.7 DU (21.5%)

303   in April (**Figure 3(d)**). The STE-sub-column negative anomaly is also not larger than for the lower tropospheric

304   sub-column in 2021, suggesting that the STE reduction had a smaller impact on the negative lower tropospheric sub-

305   column anomalies seen in 2021, in comparison with 2020.

306
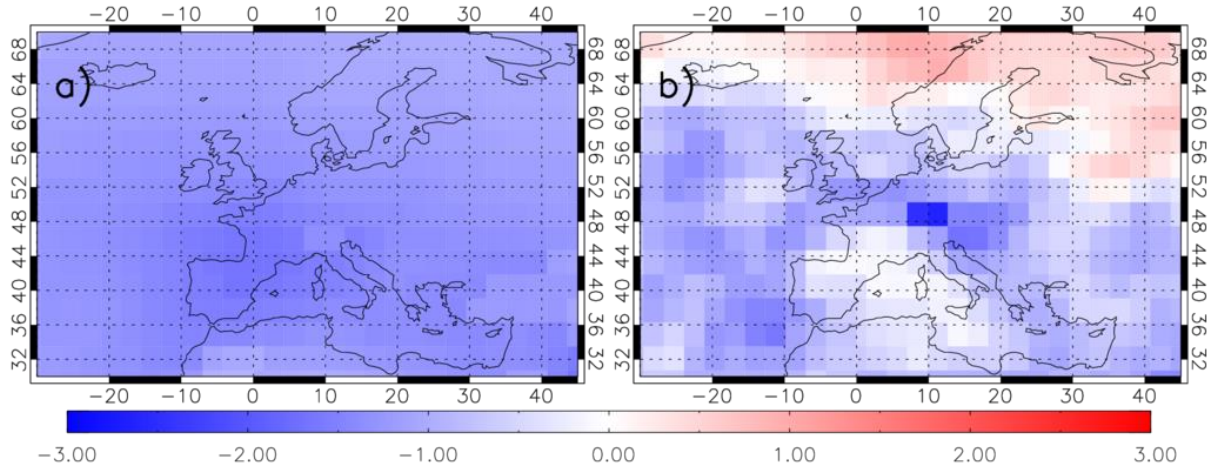
307 **Figure 4**: TOMCAT lower tropospheric ozone (DU) differences (March-May 2020 average) between a) the

308 TOMCAT COVID and TOMCAT BAU simulations and b) the TOMCAT COVID simulation with 2017-2019

309 average meteorology (TOMCAT run for 2017, 2018 and 2019 with 2020 COVID emissions and the three

310 simulations averaged together) and the TOMCAT BAU simulation.

311

312   To further quantify the relative contributions, the difference between the anomalies for the BAU and COVID

313   scenario as a relative percentage of the COVID scenario for 2020 (i.e. $100 \times$ (BAU - COVID)/COVID) is shown in

314   **Figure 5(a)**. We performed this quantification for spring-summer months showing a negative anomaly in both

315   scenarios (March–August 2020 and March–June 2021). These values represent the percentage contributions of the

316   emission reductions (due to COVID-19) and meteorological conditions to the determined reduction in the lower

317   tropospheric column zone. The contribution of emissions to the COVID scenario in spring-summer 2020 is 53%

318   (March), 67% (April), 59% (May), 71% (June), 55% (July) and 87% (August), with an average of 65% across these

319   months. Therefore, scaling the emissions is the dominant influence during this period. In 2021, the COVID scenario

320   also shows large negative anomalies, peaking at 2.2 DU (9.6%) in May. Scaling the emissions contributed towards

321   86%, 48%, 47% and 80% for March–June, respectively, of the scaled negative anomaly (average of 65%), with the

322   rest due to meteorology (and BAU emissions).

323

324

325

Figure 5. Contribution of scaled emissions and meteorology/BAU emissions to the TOMCAT lower tropospheric sub-column O_3 reduction from March–August in (a) 2020 and (b) 2021. The total reduction (DU) is the COVID scenario negative anomaly, with the relative contribution of meteorology/BAU emissions shown in orange and the contribution of scaled emissions shown in blue. The percentage relative contribution is labelled onto each bar section.

4 Conclusions

Our study represents one of the first extended investigations of the COVID-19 pandemic impacts on European lower tropospheric O_3 (surface-450 hPa) using satellite observations and modelling. The records from the Global Ozone Monitoring Experiment (GOME – 2) and the Infrared Atmospheric Sounding Interferometer (IASI) on MetOp-B show substantial decreases in European average spring-summer time lower tropospheric ozone of typically 2.0-3.0 DU (or 11.0-14.6%). While not the key focus of this paper, the 2022 decline in O_3 is interestingly the largest between 2020 and 2023. Therefore, this would suggest other factors not investigated in this study are driving a more substantial O_3 decrease and that the reported COVID-19 response is within the more extreme variability of European ozone.

To investigate the drivers of the O_3 decreases over Europe during the COVID-19 period (2020-2021), activity scaling factors (i.e. based on anonymised mobility data from big tech firms) were used to perturb the model's business-as-usual (BAU) emissions for 2020 and 2021 to quantify the COVID-19 impact on O_3. Here, the TOMCAT simulations of lower tropospheric O_3 were reduced by 2.0-3.0 DU (comparable to the O_3 reductions

345 reported by the satellite records) in the COVID-19 simulation compared to the BAU baseline. Further model

346 sensitivity experiments were able to diagnose the contribution of 2020 emissions changes (approximately 66%) and

347 2020 meteorological conditions (approximately 34%) to the overall TOMCAT simulated O_3 reduction in Europe.

348 Therefore, the COVID-19 reduced in O_3 precursor emissions were substantial in reducing 2020 European O_3, but it

349 was amplified by meteorological conditions that year. Investigation of the TOMCAT stratospheric O_3 tagged tracer

350 (i.e. a representation of the flux of stratospheric rich O_3 air into the troposphere) suggested a substantial drop in its

351 contribution to lower tropospheric O_3 (in the order of 1.0 DU), which was comparable to the meteorological signal.

352 Thus, a likely cause of the amplified European O_3 reduction in the COVID-19 period.

353 Therefore, our study has successfully quantified the impact of COVID-19 on European lower tropospheric ozone

354 and identified a useful methodology to isolate the impact of emission changes, but also importantly meteorological

355 variability, on observed changes in tropospheric composition. Future work would focus on the large reduction in

356 European O_3 in 2022 (which is beyond the scope of this study), produce a harmonised IASI O_3 record from the three

357 MetOp satellites and a reprocessing of the RAL Space GOME-2 record to more accurately account for UV-

358 degradation in the instrument record.

359

365 **Data Availability**

366 The IASI-IMS and GOME-2 data is available via the NERC Centre for Environmental Data Analysis (CEDA)

367 Jasmin platform subject to data requests. However, the IASI-IMS data and TOMCAT simulations used in this study

368 are available on Zenodo at https://zenodo.org/records/10424302 (Pimlott et al., 2024).

369 **Author Contributions**

370 MAP and RJP conceptualised, planned and undertook the research study. BJK, RS, BGL and LJV provided the data

371 and advice on using the products. MAP performed the TOMCAT model simulations with support from MPC and

372 WF. MAP prepared the manuscript with contributions from all co-authors.

373 **Conflicts of Interest**

374 The authors declare no conflicts of interest.

375

376 **References**

377 Bouarar, I., Gaubert, B., Brasseur, G. P., Steinbrecht, W., Doumbia, T., Tilmes, S., et al. (2021). Ozone Anomalies

378   in the Free Troposphere During the COVID-19 Pandemic. *Geophysical Research Letters*, *48*(16), 1–11.

379   https://doi.org/10.1029/2021GL094204

380 Callies, J., Corpaccioli, E., Eisinger, M., Hahne, A., & Lefebvre, A. (2000). GOME-2-Metop's second-generation

381 sensor for operational ozone monitoring. *ESA Bulletin*, *102*(may), 28–36.

382 Chang, K. L., Cooper, O. R., Gaudel, A., Allaart, M., Ancellet, G., Clark, H., et al. (2022). Impact of the COVID-19

383 Economic Downturn on Tropospheric Ozone Trends: An Uncertainty Weighted Data Synthesis for

384 Quantifying Regional Anomalies Above Western North America and Europe. *AGU Advances*, *3*(2).

385 https://doi.org/10.1029/2021AV000542

386 Chipperfield, M. P. (2006). New version of the TOMCAT/SLIMCAT off-line chemical transport model:

387 Intercomparison of stratospheric tracer experiments. *Quarterly Journal of the Royal Meteorological Society*,

388 *132*(617), 1179–1203. https://doi.org/10.1256/qj.05.51

389 Clark, H., Bennouna, Y., Tsivlidou, M., Wolff, P., Sauvage, B., Barret, B., et al. (2021). The effects of the COVID-

390 19 lockdowns on the composition of the troposphere as seen by In-service Aircraft for a Global Observing

391 System (IAGOS) at Frankfurt. *Atmospheric Chemistry and Physics*, *21*(21), 16237–16256.

392 https://doi.org/10.5194/acp-21-16237-2021

393 Clerbaux, C., Boynard, A., Clarisse, L., George, M., Hadji-Lazaro, J., Herbin, H., et al. (2009). Monitoring of

394 atmospheric composition using the thermal infrared IASI/MetOp sounder. *Atmospheric Chemistry and*

395 *Physics*, *9*(16), 6041–6054. https://doi.org/10.5194/acp-9-6041-2009

396 Cuesta, J., Costantino, L., Beekmann, M., Siour, G., Menut, L., Bessagnet, B., et al. (2022). Ozone pollution during

397 the COVID-19 lockdown in the spring of 2020 over Europe, analysed from satellite observations, in situ

398 measurements, and models. *Atmospheric Chemistry and Physics*, *22*(7), 4471–4489.

399 https://doi.org/10.5194/acp-22-4471-2022

400 Doumbia, T., Granier, C., Elguindi, N., Bouarar, I., Darras, S., Brasseur, G., et al. (2021). Changes in global air

401 pollutant emissions during the COVID-19 pandemic: A dataset for atmospheric modeling. *Earth System*

402 *Science Data*, *13*(8), 4191–4206. https://doi.org/10.5194/essd-13-4191-2021.

403 Dunn, R. J. H., J. Blannin, N. Gobron, J. B Miller, and K. M. Willett, Eds., 2024: Global Climate [in "State of the

404 Climate in 2023"]. Bull. Amer. Meteor. Soc., 105 (8), S12–S155, https://doi.org/10.1175/BAMS-D24-

405 0116.1.European Environment Agency. (2022). *Air quality in Europe 2022*. https://doi.org/10.2800/488115

406 Feng, L., Smith, S. J., Braun, C., Crippa, M., Gidden, M. J., Hoesly, R., et al. (2020). The generation of gridded

407 emissions data for CMIP6. *Geoscientific Model Development*, *13*(2), 461–482. https://doi.org/10.5194/gmd-

408 13-461-2020

409 Feng, W., Dhomse, S. S., Arosio, C., Weber, M., Burrows, J. P., Santee, M. L., & Chipperfield, M. P. (2021). Arctic

410 Ozone Depletion in 2019/20: Roles of Chemistry, Dynamics and the Montreal Protocol. *Geophysical*

411 *Research Letters*, *48*(4), 1–10. https://doi.org/10.1029/2020GL091911

412 Forster, P. M., Forster, H. I., Evans, M. J., Gidden, M. J., Jones, C. D., Keller, C. A., et al. (2020). Current and

413 future global climate impacts resulting from COVID-19. *Nature Climate Change*, *10*(10), 913–919.

414 https://doi.org/10.1038/s41558-020-0883-0

415 Gidden, M. J., Riahi, K., Smith, S. J., Fujimori, S., Luderer, G., Kriegler, E., et al. (2019). Global emissions

416 pathways under different socioeconomic scenarios for use in CMIP6: a dataset of harmonized emissions

417 trajectories through the end of the century. *Geoscientific Model Development*, *12*(4), 1443–1475.

418 https://doi.org/10.5194/gmd-12-1443-2019

419 Grange, S. K., Lee, J. D., Drysdale, W. S., Lewis, A. C., Hueglin, C., Emmenegger, L., & Carslaw, D. C. (2021).

420 COVID-19 lockdowns highlight a risk of increasing ozone pollution in European urban areas. *Atmospheric*

421 *Chemistry and Physics*, *21*(5), 4169–4185. https://doi.org/10.5194/acp-21-4169-2021

422 Guevara, M., Jorba, O., Soret, A., Petetin, H., Bowdalo, D., Serradell, K., et al. (2021). Time-resolved emission

423 reductions for atmospheric chemistry modelling in Europe during the COVID-19 lockdowns. *Atmospheric*

424 *Chemistry and Physics*, *21*(2), 773–797. https://doi.org/10.5194/acp-21-773-2021

425 Hersbach, H., Bell, B., Berrisford, P., Hirahara, S., Horányi, A., Muñoz-Sabater, J., et al. (2020). The ERA5 global

426 reanalysis. *Quarterly Journal of the Royal Meteorological Society*, *146*(730), 1999–2049.

427 https://doi.org/10.1002/qj.3803

428 IPCC. (2021). *Climate Change 2021: The Physical Science Basis: Contribution of Working Group I to the Sixth*

429 *Assessment Report of the Intergovernmental Panel on Climate Change*. (V. Masson-Delmotte, P. Zhai, A.

430 Pirani, S. L. Connors, C. Péan, S. Berger, et al., Eds.). Cambridge, United Kingdom: Cambridge University

431 Press. https://doi.org/10.1017/9781009157896

432 Mann, G. W., Carslaw, K. S., Spracklen, D. V., Ridley, D. A., Manktelow, P. T., Chipperfield, M. P., et al. (2010).

433 Description and evaluation of GLOMAP-mode: A modal global aerosol microphysics model for the UKCA

434 composition-climate model. *Geoscientific Model Development*, *3*(2), 519–551. https://doi.org/10.5194/gmd-3-

435 519-2010

436 Miles, G. M., Siddans, R., Kerridge, B. J., Latter, B. G., & Richards, N. A. D. (2015). Tropospheric ozone and

437 ozone profiles retrieved from GOME-2 and their validation. *Atmospheric Measurement Techniques*, *8*(1),

438 385–398. https://doi.org/10.5194/amt-8-385-2015

439 Miyazaki, K., Bowman, K., Sekiya, T., Takigawa, M., Neu, J. L., Sudo, K., et al. (2021). Global tropospheric ozone

440 responses to reduced NOx emissions linked to the COVID-19 worldwide lockdowns. *Science Advances*, *7*(24),

441 1–15. https://doi.org/10.1126/sciadv.abf7460

442 Monks, P. S., Archibald, A. T., Colette, A., Cooper, O., Coyle, M., Derwent, R., et al. (2015). Tropospheric ozone

443 and its precursors from the urban to the global scale from air quality to short-lived climate forcer. *Atmospheric*

444 *Chemistry and Physics*, *15*(15), 8889–8973. https://doi.org/10.5194/acp-15-8889-2015

445 Monks, S. A., Arnold, S. R., Hollaway, M. J., Pope, R. J., Wilson, C., Feng, W., et al. (2017). The TOMCAT global

446 chemical transport model v1.6: Description of chemical mechanism and model evaluation. *Geoscientific*

447 *Model Development*. https://doi.org/10.5194/gmd-10-3025-2017

448 Munro, R., Lang, R., Klaes, D., Poli, G., Retscher, C., Lindstrot, R., et al. (2016). The GOME-2 instrument on the

449 Metop series of satellites: Instrument design, calibration, and level 1 data processing - An overview.

450 *Atmospheric Measurement Techniques*, *9*(3), 1279–1301. https://doi.org/10.5194/amt-9-1279-2016

451 Ordóñez, C., Garrido-Perez, J. M., & García-Herrera, R. (2020). Early spring near-surface ozone in Europe during

452 the COVID-19 shutdown: Meteorological effects outweigh emission changes. *Science of the Total*

453 *Environment*, *747*(December 2019), 141322. https://doi.org/10.1016/j.scitotenv.2020.141322

454 Parrish, D. D., Derwent, R. G., Faloona, I. C., & Mims, C. A. (2022). Technical note: Northern midlatitude baseline

ozone - Long-term changes and the COVID-19 impact. *Atmospheric Chemistry and Physics*, *22*(20), 13423–13430. https://doi.org/10.5194/acp-22-13423-2022

Pey, J., & Cerro, J. C. (2022). Reasons for the observed tropospheric ozone weakening over south-western Europe during COVID-19: Strict lockdown versus the new normal. *Science of the Total Environment*, *833*(March). https://doi.org/10.1016/j.scitotenv.2022.155162

Pimlott, M. A., Pope, R. J., Kerridge, B. J., Siddans, R., Latter, B. G., Ventress, L. J., et al. (2024). TOMCAT model data & IASI/GOME-2B satellite data of European ozone between 2008 - 2023. Zenodo. https://doi.org/doi.org/10.5281/zenodo.10424302

Pope, R. J., Arnold, S. R., Chipperfield, M. P., Reddington, C. L. S., Butt, E. W., Keslake, T. D., et al. (2020). Substantial increases in Eastern Amazon and Cerrado biomass burning-sourced tropospheric ozone. *Geophysical Research Letters*, 47, e2019GL084143. https://doi.org/10.1029/2019GL084143.

Pope, R J, Kerridge, B. J., Chipperfield, M. P., Siddans, R., Latter, B. G., Ventress, L. J., et al. (2023). Investigation of the summer 2018 European ozone air pollution episodes using novel satellite data and modelling. *Atmospheric Chemistry and Physics*, *23*(20), 13235–13253. https://doi.org/10.5194/acp-23-13235-2023

Pope, Richard J., Kerridge, B. J., Siddans, R., Latter, B. G., Chipperfield, M. P., Arnold, S. R., et al. (2021). Large enhancements in southern hemisphere satellite-observed trace gases due to the 2019/2020 Australian wildfires. *Journal of Geophysical Research: Atmospheres*, 1–13. https://doi.org/10.1029/2021jd034892

Pope, R. J., Rap, A., Pimlott, M. A., Barret, B., Le Flochmoen, E., Kerridge, B. J., Siddans, R., Latter, B. G., Ventress, L. J., Boynard, A., Retscher, C., Feng, W., Rigby, R., Dhomse, S. S., Wespes, C., and Chipperfield, M. P.: Quantifying the tropospheric ozone radiative effect and its temporal evolution in the satellite era, Atmos. Chem. Phys., 24, 3613–3626, https://doi.org/10.5194/acp-24-3613-2024, 2024.

Putero, D., Cristofanelli, P., Chang, K.-L., Dufour, G., Beachley, G., Couret, C., Effertz, P., Jaffe, D. A., Kubistin, D., Lynch, J., Petropavlovskikh, I., Puchalski, M., Sharac, T., Sive, B. C., Steinbacher, M., Torres, C., and Cooper, O. R.: Fingerprints of the COVID-19 economic downturn and recovery on ozone anomalies at high-elevation sites in North America and western Europe, Atmos. Chem. Phys., 23, 15693–15709, https://doi.org/10.5194/acp-23-15693-2023, 2023.Riahi, K., van Vuuren, D. P., Kriegler, E., Edmonds, J., O'Neill, B. C., Fujimori, S., et al. (2017). The Shared Socioeconomic Pathways and their energy, land use, and greenhouse gas emissions implications: An overview. *Global Environmental Change*, *42*, 153–168. https://doi.org/https://doi.org/10.1016/j.gloenvcha.2016.05.009

Richards, N. A. D., Arnold, S. R., Chipperfield, M. P., Miles, G., Rap, A., Siddans, R., et al. (2013). The Mediterranean summertime ozone maximum: Global emission sensitivities and radiative impacts. *Atmospheric Chemistry and Physics*, *13*(5), 2331–2345. https://doi.org/10.5194/acp-13-2331-2013.

Rowlinson, M. J., Rap, A., Arnold, S. R., Pope, R. J., Chipperfield, M. P., McNorton, J., Forster, P., Gordon, H., Pringle, K. J., Feng, W., Kerridge, B. J., Latter, B. L., and Siddans, R.: Impact of El Niño–Southern Oscillation on the interannual variability of methane and tropospheric ozone, Atmos. Chem. Phys., 19, 8669–8686, https://doi.org/10.5194/acp-19-8669-2019, 2019.

Skeie, R. B., Myhre, G., Hodnebrog, Ø., Cameron-Smith, P. J., Deushi, M., Hegglin, M. I., et al. (2020). Historical total ozone radiative forcing derived from CMIP6 simulations. *Npj Climate and Atmospheric Science*, *3*(1). https://doi.org/10.1038/s41612-020-00131-0

494   Spracklen, D. V., Pringle, K. J., Carslaw, K. S., Chipperfield, M. P., & Mann, G. W. (2005). A global off-line model

495   of size-resolved aerosol microphysics: I. Model development and prediction of aerosol properties.

496   *Atmospheric Chemistry and Physics*, *5*(8), 2227–2252. https://doi.org/10.5194/acp-5-2227-2005

497   Steinbrecht, W., Kubistin, D., Plass-Dülmer, C., Davies, J., Tarasick, D. W., Von Der Gathen, P., et al. (2021).

498   COVID-19 Crisis Reduces Free Tropospheric Ozone Across the Northern Hemisphere. *Geophysical Research*

499   *Letters*, *48*(5), 1–11. https://doi.org/10.1029/2020GL091987

500   Weber, M., Arosio, C., Feng, W., Dhomse, S. S., Chipperfield, M. P., Meier, A., et al. (2021). The Unusual

501   Stratospheric Arctic Winter 2019/20: Chemical Ozone Loss From Satellite Observations and TOMCAT

502   Chemical Transport Model. *Journal of Geophysical Research: Atmospheres*, *126*(6), 1–14.

503   https://doi.org/10.1029/2020JD034386

504   WHO. (2020). Naming the coronavirus disease (COVID-19) and the virus that causes it. Retrieved April 14, 2023,

505   from https://www.who.int/emergencies/diseases/novel-coronavirus-2019/technical-guidance/naming-the-

506   coronavirus-disease-(covid-2019)-and-the-virus-that-causes-it

507   Wohltmann, I., von der Gathen, P., Lehmann, R., Maturilli, M., Deckelmann, H., Manney, G. L., et al. (2020). Near-

508   Complete Local Reduction of Arctic Stratospheric Ozone by Severe Chemical Loss in Spring 2020.

509   *Geophysical Research Letters*, *47*(20). https://doi.org/10.1029/2020GL089547

510   Young, P. J., Archibald, A. T., Bowman, K. W., Lamarque, J.-F., Naik, V., Stevenson, D. S., Tilmes, S.,

511   Voulgarakis, A., Wild, O., Bergmann, D., Cameron-Smith, P., Cionni, I., Collins, W. J., Dalsøren, S. B., Doherty, R.

512   M., Eyring, V., Faluvegi, G., Horowitz, L. W., Josse, B., Lee, Y. H., MacKenzie, I. A., Nagashima, T., Plummer, D.

513   A., Righi, M., Rumbold, S. T., Skeie, R. B., Shindell, D. T., Strode, S. A., Sudo, K., Szopa, S., and Zeng, G.: Pre-

514   industrial to end 21st century projections of tropospheric ozone from the Atmospheric Chemistry and Climate Model

515   Intercomparison Project (ACCMIP), Atmos. Chem. Phys., 13, 2063–2090, https://doi.org/10.5194/acp-13-2063-

516   2013, 2013.

517   Zhou, P., Yang, X. Lou, Wang, X. G., Hu, B., Zhang, L., Zhang, W., et al. (2020). A pneumonia outbreak associated

518   with a new coronavirus of probable bat origin. *Nature*, *579*(7798), 270–273. https://doi.org/10.1038/s41586-

519   020-2012-7

520   Ziemke, J. R., Kramarova, N. A., Frith, S. M., Huang, L. K., Haffner, D. P., Wargan, K., et al. (2022). NASA

521   Satellite Measurements Show Global-Scale Reductions in Free Tropospheric Ozone in 2020 and Again in

522   2021 During COVID-19. *Geophysical Research Letters*, *49*(15). https://doi.org/10.1029/2022GL098712